

# Anodic Oxidation of Titanium in Mixture of $\beta$ -Glycerophosphate ( $\beta$ -GP) and Calcium Acetate (CA)

H.Z. Abdullah<sup>1, a</sup>, P. Koshy<sup>2, b</sup> and C.C. Sorrell<sup>2, c</sup>

<sup>1</sup>Faculty of Mechanical and Manufacturing, Universiti Tun Hussein Onn Malaysia,  
86400 Parit Raja, Batu Pahat, Johor, Malaysia

<sup>2</sup>School of Materials Science and Engineering, University of New South Wales, Sydney,  
NSW 2052, Australia

<sup>a</sup>hasan@uthm.edu.my, <sup>b</sup>koshy@unsw.edu.au, <sup>c</sup>c.sorrell@unsw.edu.au

**Keywords:** Titanium, Titania, Anodic oxidation, Glancing angle X-ray diffraction, Colour

**Abstract.** Anodic oxidation is an electrochemical method for the production of a ceramic film on a metallic substrate. It involves the use of an electrical bias at relatively low currents while the substrate is immersed in a weak organic acid bath. The films produced are usually dense and stable, with variable microstructural features. In the present work, ceramic films of the anatase and rutile polymorphs of TiO<sub>2</sub> were formed on high-purity Ti foil (50  $\mu$ m) using mixtures of  $\beta$ -glycerophosphate disodium salt pentahydrate ( $\beta$ -GP) and calcium acetate monohydrate (CA) solutions. The experiments were carried out at varying voltages (150-350 V), times (1-10 min), and current density (10 mA.cm<sup>-2</sup>) at room temperature. The ceramic films were characterised using digital photography, glancing angle X-ray diffraction (GAXRD), and field emission scanning electron microscopy (FESEM). The thicknesses of the films on Ti were measured using focused ion beam (FIB) milling. The colour, microstructures, and thicknesses of the films were seen to be strongly dependent on the applied voltage. At bias <200 V, single-phase anatase was observed to form on Ti, while at higher bias (250 V), rutile formed due to the arcing process.

## Introduction

Anodic oxidation is used to modify the surface characteristics and properties of titanium and aluminum in order to improve the mechanical properties, corrosion resistance, biocompatibility and to eliminate the biotoxicity [1-6]. Anodic oxidation of titanium allows for the controlled formation of a protective oxide surface layer which is much thicker than that formed naturally. These coatings may be dense or porous, and/or amorphous or crystalline, depending on the parameters such as electrolyte type, solution concentration, and applied potential [7,8]. Titanium is naturally covered by a 1.5-10 nm oxide passive layer [9]. By modifying the surface in  $\beta$ -GP + CA electrolyte, the thickness (>1 $\mu$ m) [10] and mineralogy of the oxide can be controlled. The CA +  $\beta$ -GP electrolyte was used due to the ion of calcium and phosphorous which is embedded in the titanium surface during anodizing [11]. Anodising in only  $\beta$ -GP electrolyte produces a smooth surface even when a voltage of 300 V is used [10]. By adding CA in  $\beta$ -GP, a rough and porous oxide layer can be formed. The roughness of the surface is one of the main properties of the implant. CA mixed with  $\beta$ -GP has been used as an electrolyte for the anodising of titanium because of their roles in modifying the surface of titanium and in promoting bone tissue growth and enhanced anchorage of the implant to bone [12]. The advantages of this method include: (1) excellent control of the thickness of the oxide layer formed on titanium surface [13]; (2) ease of uniform applicability over surfaces with complex geometries such as screws and dental applications [12,14]; (3) variability in the properties of the oxide surface formed (rough and porous) [10] and (4) short process times [15].

## Experimental Procedure

**Sample Preparation.** High-purity titanium foils of dimensions 25 mm x 10 mm x 0.5 mm were wet hand-polished using 1200 grit (~1  $\mu$ m) abrasive paper, and then immersed in an ultrasonic bath with acetone, rinsed with distilled water, and then dried using compressed air.

**Anodisation.** Anodic oxidation was carried out in an electrochemical cell containing ~0.4 L of a mixture made from aqueous solutions of  $\beta$ -GP (Fluka,  $\geq 98.0\%$ ) and CA (Fluka,  $\geq 90.0\%$ ) at  $\sim 25^\circ\text{C}$  [1,8]. These experimental parameters used are shown in Table 1. The anode and cathode were titanium foil and the anodising was done with a programmable power supply (EC2000P, E-C Apparatus Corp., USA). The anodised foils were cleaned by dipping in distilled water, followed by drying in air.

Table 1. Parameters used for anodic oxidation in  $\beta$ -GP + CA.

| Parameter  | Value(s)                           |
|--|------------------------------------|
| Electrolytes                                       | 0.04 M $\beta$ -GP + 0.4 M CA [11] |
| d.c. Voltage (V)                                   | 150, 200, 250, 300, 350            |
| Current Density ( $\text{mA}\cdot\text{cm}^{-2}$ ) | 10 [11]                            |
| Duration (min)                                     | 1, 3, 5, 10                        |

**Characterisation.** The mineralogical composition of the films was determined using glancing angle X-ray diffraction (XRD, Philips X'Pert PRO Materials Research Diffraction System) at 45 kV and 40 mA, angle of incidence of  $0.8^\circ$ , scanning speed of  $0.01^\circ 2\theta/\text{s}$ , and step size of  $0.02^\circ 2\theta$ . The microstructures were examined using a FESEM (Hitachi, Model S4500 II) at an accelerating voltage of 20 kV. The colour was recorded using a digital camera (Olympus  $\mu 725\text{SW}$ ). FIB (FEI xP200) milling was used for cross-sectional imaging.

## Results and Discussion

**Colour of Anodic Films:** It is known that titanium metal when exposed to atmosphere is anodised to form a passive film of 1.5-10 nm thickness, which has no colour. By increasing the thickness of the oxide film, the colour changes as a result of interference effects. According to multiple-beam theory, the colouring results from the interference between the light beams that are reflected from the (a) film surface and (b) film-substrate interface [16]. In this study, the colour variation was correlated with the applied voltages, anodisation times, and current densities. The influence of the applied voltage and the anodisation time on the colour of the films was analysed from the images captured using a digital camera. Fig. 1 shows the colour of the oxide films produced at the current density of  $10 \text{ mA}\cdot\text{cm}^{-2}$ . The colour of the oxide films in Fig. 1 can be categorised into three groups based on arcing and its effects:

1. Non-Arcing            Light green and light chocolate-purple
2. Arcing                Light green and grey
3. Rutile Formation    Grey

| Voltage (V) | Anodisation Time (min) |   |        |                  |
|-------------|------------------------|---|--------|------------------|
|             | 1                      | 3 | 5      | 10               |
| 150         | Non-Arcing             |   |        |                  |
| 200         |                        |   |        |                  |
| 250         |                        |   | Arcing |                  |
| 300         |                        |   |        | Rutile Formation |
| 350         |                        |   |        |                  |

Fig. 1. Colour of film surfaces ( $10 \text{ mA}\cdot\text{cm}^{-2}$ ) as a function of the applied voltage and the anodisation time.

The use of a higher current density resulted in a greater intensity of arcing. This is due to the higher conductivity in the solution and the localised heating from the arcing, which raised the temperature. At the higher temperature, phase transformation to rutile occurred. The data show that the arcing process is associated with the generation of a grey colour, which probably results from partial reduction due to localised melting [17,18].

**Glancing Angle X-Ray Diffraction:** The GAXRD patterns of the anodised samples obtained under various voltages and anodisation times at the lower current density of  $10 \text{ mAcm}^{-2}$  are shown in Fig. 2 and Fig. 3. These data show the following trends (Table 2):

Table 2. Explanation of GAXRD for Fig. 2 and Fig. 3.

| 150 V / 1-10 min                                    | 350 V / 1-10 min                           |
|---|--|
| Very small effect of anodisation time (after 3 min) | Clear effect of anodisation time           |
| Small amount of anatase                             | Larger amount of anatase                   |
| Very low amount of rutile at 10 min only            | Noticeable amount of rutile at 10 min only |

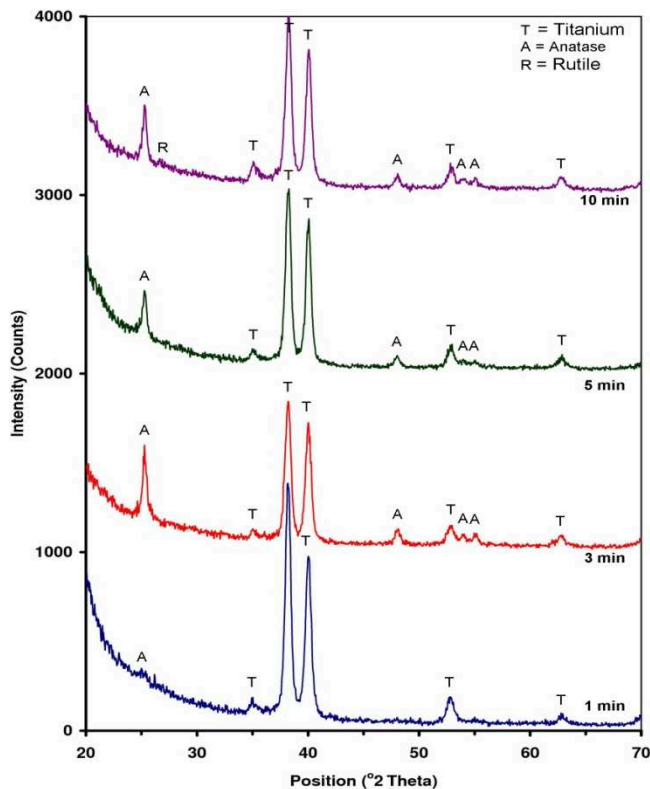


Fig. 2. GAXRD patterns of the anodised samples ( $10 \text{ mA.cm}^{-2}$ ) at 150 V for 1, 3, 5, and 10 min.

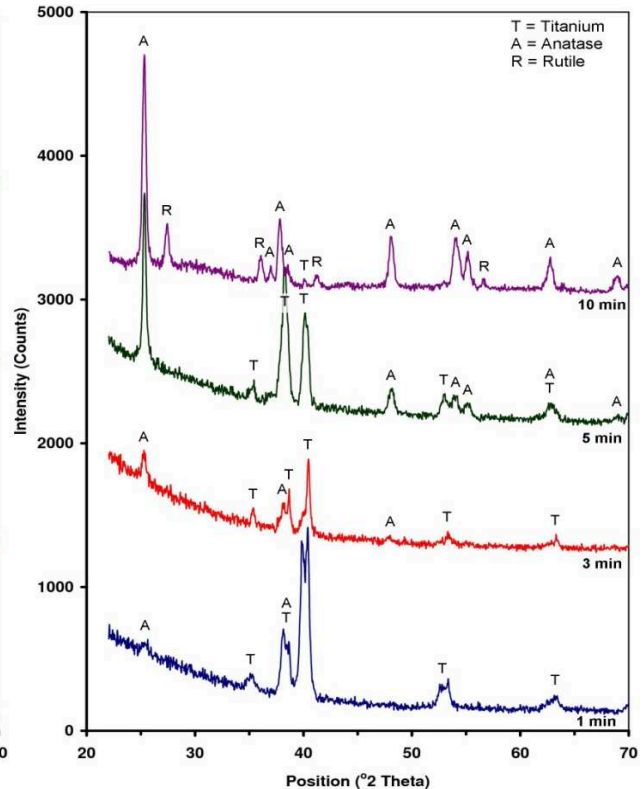


Fig. 3. GAXRD patterns of the anodised samples ( $10 \text{ mA.cm}^{-2}$ ) at 350 V for 1, 3, 5, and 10 min.

The current density has an effect on rutile formation, which is expected since the formation of this phase is facilitated by arcing. Even very low applied voltages (as low as  $\sim 10 \text{ V}$ ) have been observed to facilitate the transition of amorphous titania to crystalline anatase [19]. This recrystallisation is considered to result from the electrical conductivity and oxygen mobility associated with the liquid electrolyte [20]. According to Kuromoto *et al.*, [21], at high voltages  $\text{TiO}_2$  films are formed due to the inward migration of  $\text{O}^{2-}$  ions to the metal/film interface and the outward migration of  $\text{Ti}^{4+}$  ions from metallic Ti to the film/electrolyte interface. Following this reasoning, the only reason for  $\text{Ti}^{4+}$  migration is charge balance within the crystalline  $\text{TiO}_2$  (high voltage). Since  $\text{TiO}_2$  is known to be oxygen-deficient ( $\text{TiO}_{2-z}$ ), the oxygen surplus from the electrolyte cannot be accommodated in the oxide, and this implies that charge balance is required, i.e., if oxygen injection in  $\text{TiO}_2$  occurs, then titanium injection must occur to compensate. A simple schematic of the process is shown in Fig. 4.

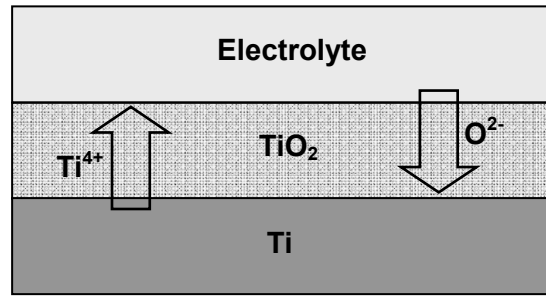


Fig. 4. Schematic illustrating the formation of crystalline oxide in an anodic film on titanium

At high applied voltages, arcing is initiated at a potential above the breakdown voltage, resulting in the developed of micro-arcs which are extinguished very rapidly (within  $10^{-4}$ - $10^{-5}$  s) [15]. In spite of this short time frame, considerable localised heating occurs, leading to high temperatures ( $10^4$  °C), and additionally very high pressures also are generated ( $10^2$ - $10^3$  MPa) [22]. These conditions are sufficient to initiate reactions between the substrate and the electrolyte. The resultant oxide films that grow by the arcing process move rapidly across the titanium surface (anode).

**Scanning Electron Microscopy:** Fig. 5 shows FESEM images of the anodic films as a function of applied voltage, time, and current density.

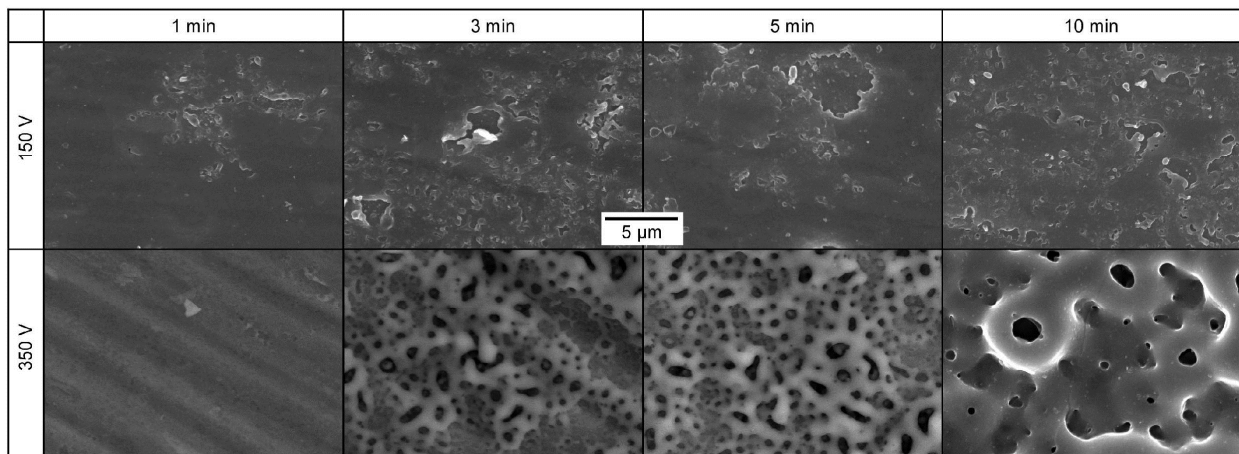


Fig. 5. FESEM micrographs of anodised surfaces ( $10 \text{ mA}\cdot\text{cm}^{-2}$ ) at 150 V and 350 V for 1, 3, 5 and 10 min.

From these data, the following observations can be made with regard to the effect of the different parameters, as summarised below:

1. The number of pores increases with increasing applied voltage.
2. The surface profile becomes more uneven at higher applied voltages, which is a reflection of the increased porosity and the raised profile of the pore crater
3. The pore size increases with increasing applied voltage, which is a reflection of the intensity of the arcing and the consequent melting and shrinkage.
4. Cracking is enhanced with higher applied voltages owing to possible shrinkage stresses and thermal shock.
5. Rutile formation generally is enhanced with increasing the voltage and time owing to energetic considerations.
6. The extent of melting as a function of applied voltage is indicated by the decrease in the visibility of grain boundaries (surface homogeneity).

Generally, the dominant cause of pore generation is increasing applied voltage, which enhances the arcing at the metal/titania interface, thereby increasing the pore size (up to  $\sim 5 \mu\text{m}$  in diameter). Sul *et al.* [9] have attributed the presence of large pores to the interconnection of smaller pores with one another.

**Cross-Section Focused Ion Beam (FIB) Milling:** Fig. 6 shows the FIB images of the top view and cross-section tilted at 45° of the samples, at 10 mA.cm<sup>-2</sup> current density for 10 min at the highest voltage. From the cross-sectional images, the following features can be seen:

1. The maximal thickness of the films can be seen to be ~3.0 μm. The thickness obviously was variable owing to the presence of the pores.
2. The film thickness is comprised of three sections:
  - (a) Dense outer oxide layer, which formed prior to arcing and consists of amorphous titania
  - (b) Large, discontinuous, elongated, subsurface pores (~1 μm thickness) created by the coalescence of small pores formed by arcing
  - (c) Small subsurface pores of ~1 μm thickness, adjacent to the metal surface
3. The titania layer is intimately bonded to the metal surface, as noted previously [12].

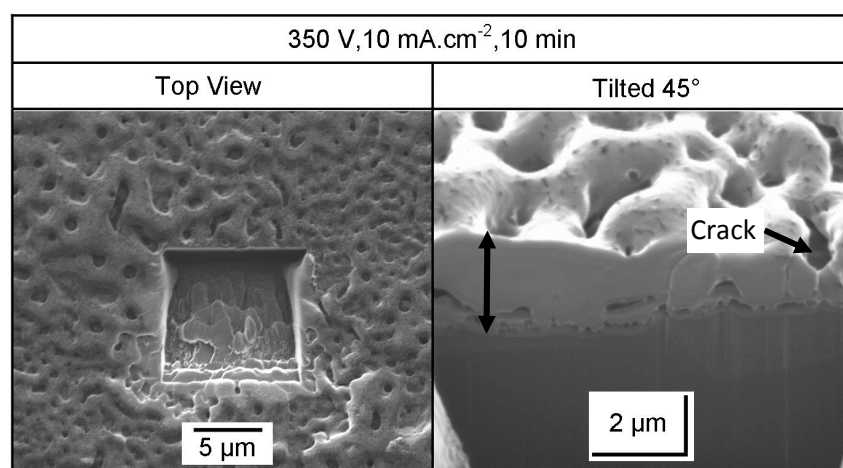


Fig. 6. FIB micrographs showing the cross sectional regions for anodised samples at 10 mA.cm<sup>-2</sup> for 10 min.

Fig. 6 shows cracks present on the surface and throughout the oxide layer during anodising at the highest applied voltages (300 V and 350 V). These cracks can cross into the dense outer oxide layer. As indicated before, cracks can occur due to thermal gradients established during and after arcing [15]. At higher voltages (450 V and 500 V), the anodised layer can react with elements in the electrolyte to form more complex oxides [10]. At these voltages, the anodised layer was observed to contain  $\beta$ -Ca<sub>2</sub>P<sub>2</sub>O<sub>7</sub>, CaTiO<sub>3</sub>,  $\alpha$ -Ca<sub>3</sub>(PO<sub>4</sub>)<sub>2</sub>, and Ca<sub>2</sub>Ti<sub>5</sub>O<sub>12</sub> [21,12].

## Conclusions

Anodic oxidation of titanium in weak organic acids (CA +  $\beta$ -GP) can be summaries as below:

- Anodisation in weak organic acids can be controlled more easily to produce oxide layers (anatase and/or rutile) on the Ti surface.
- The colour of the oxide layer was dependent on the arcing effect.
- The mineralogy of oxide layer depends on the applied voltages and anodisation times.
- The dominant cause of porosity generation is increasing applied voltage, which enhances arcing at the metal/titania interface, thereby increasing the pore size.
- The thickness of the films and subsurface pore generation are increased by increasing the applied voltage due to arcing process.

## Acknowledgements

The authors would like to thank Universiti Tun Hussein Onn Malaysia and the Ministry of Higher Education, Malaysia (Fundamental Research Grant Scheme; Vot 1212), for financial support for this work.

**References**

- [1] H.J. Oh, J.H. Lee, Y. Jeong, Y.J. Kim, and C.S. Chi: Surf. Coat. Tech. Vol. 198 (2004), p. 247.
- [2] H.M. Kim, F. Miyaji, T. Kokubo, T. Kitsugi, and T. Nakamura: J. Biomed. Mater. Res. Vol. 32 (1996), p. 409.
- [3] C.E.B. Marino, P.A.P. Nascente, S.R. Biaggio, R.C. Rocha-Filho, and N. Bocchi: Thin Solid Films Vol. 468 (2004), p. 109.
- [4] T. Kokubo, H.M. Kim, and M. Kawashita: Biomat. Vol. 24 (2003), p. 2161.
- [5] L. Jonašova, F.A. Muller, A. Helebrant, J. Strnad, and P. Greil: Biomater. Vol. 23 (2002), p. 3095.
- [6] B. Yang, M. Uchida, H.M. Kim, X. Zhang, and T. Kukobo: Biomater. Vol. 25 (2004), p. 1003.
- [7] C. Jaeggi, P. Kern, J. Michler, T. Zehnder, and H. Siegenthaler: Surf. Coat. Tech. Vol. 200 (2005), p. 1913.
- [8] H.Z. Abdullah and C.C. Sorrell: J. Aust. Ceram. Soc. Vol. 43 (2007), p. 125.
- [9] Y.T. Sul, C.B. Johanson, Y. Jeong, and T. Albrektsson: Med. Eng. Phys. Vol. 23 (2001), p. 329.
- [10] H. Ishizawa and M. Ogino: J. Biomed. Mater. Res. Vol. 29 (1995), p. 65.
- [11] H.Z. Abdullah: *Titanium surface modification by oxidation for biomedical application*, The University of New South Wales, Australia (2010).
- [12] Y. Han, S.H. Hong, and K. Xu: Surf. Coat. Tech. Vol. 168 (2003), p. 249.
- [13] H.Z. Abdullah and C.C. Sorrell: Mater. Sci. For. Vol.561-565 (2007), p. 2159.
- [14] S.J. Park: Met. and Mater. Inter. Vol. 14 (2008), p. 449.
- [15] A.L. Yerokhin, X. Nie, A. Leyland, A. Matthews, and S.J. Dowey: Surf. Coat. Tech. Vol. 122 (1999), p. 73.
- [16] J.L. Delplancke, M. Degrez, A. Fontana, and R. Winand: Surf. Tech. Vol. 16 (1982), p. 153.
- [17] H.Z. Abdullah and C.C. Sorrell: Mater. Austr. Vol. 41 (2008), p. 44.
- [18] H.Z. Abdullah and C.C. Sorrell: Adv. Mater. Res. Vol. 545 (2012), p. 223.
- [19] A. Aladjem: J. Mater. Sci. Vol. 8 (1973), p. 688.
- [20] H. Habazaki, M. Uozumi, H. Konno, K. Shimizu, P. Skeldon, G.E. Thompson: Corr. Sci. Vol. 45 (2003), p. 2063.
- [21] N.K. Kuromoto, R.A. Simão, and G.A. Soares: Mater. Charac. Vol. 58 (2007), p. 114.
- [22] W.H. Song, Y.K. Jun, Y. Han, and S.H. Hong: Biomater. Vol. 25 (2004), p. 3341.